Remote Sensing of Environment 219 (2018) 89–98

Contents lists available at ScienceDirect

Remote Sensing of Environment

journal homepage: www.elsevier.com/locate/rse

Heritable variation in needle spectral reflectance of Scots pine (*Pinus sylvestris* L.) peaks in red edge

Jaroslav Čepl[a,*], Jan Stejskal[a], Zuzana Lhotáková[b], Dana Holá[c], Jiří Korecký[a], Milan Lstibůrek[a], Ivana Tomášková[a], Marie Kočová[c], Olga Rothová[c], Markéta Palovská[c], Jakub Hejtmánek[a], Anna Krejzková[a], Salvador Gezan[d], Ross Whetten[e], Jana Albrechtová[b]

[a] Czech University of Life Sciences, Faculty of Forestry and Wood Sciences, Kamýcká 1176, 165 21 Praha 6, Suchdol, Czech Republic
[b] Charles University in Prague, Faculty of Science, Department of Experimental Plant Biology, Albertov 6, 128 43 Praha 2, Czech Republic
[c] Charles University in Prague, Faculty of Science, Department of Genetics and Microbiology, Albertov 6, 128 43 Praha 2, Czech Republic
[d] School of Forest Resources and Conservation, University of Florida, PO Box 110410, Gainesville, FL, USA
[e] Department of Forestry & Environmental Resources, North Carolina State University, Raleigh, NC 27695-8008, USA

ARTICLE INFO

Keywords:
Pedigree reconstruction
NDVI
Spectral vegetation indices
Chlorophyll
Carotenoids

ABSTRACT

Foliar reflectance is readily used in evaluating physiological status of agricultural crops and forest stands. However, in the case of forest trees, underlying genetics of foliar spectral reflectance and pigment content have rarely been investigated. We studied a structured population of Scots pine, replicated on two sites, with the selected trees´ pedigree reconstructed via DNA markers. This allowed us to decompose phenotypic variance of pigment and reflectance traits into its causal genetic components, and to estimate narrow-sense heritability (h^2).

We found statistically significant h^2 ranging from 0.07 to 0.22 for most of the established reflectance indices. Additionally, we investigated the profile of heritable variation along the reflectance curve in 1 nm wavelength (WL) bands. We show that the maximum h^2 value (0.39; SE 0.13) across the 400 to 2500 nm spectral range corresponds to the red edge inflection point, in this case to 722 nm WL band. Resultant h^2 distribution indicates that additive gene effects fluctuate along the reflectance curve.

Furthermore, h^2 of the most widely used formats of reflectance indices, i.e. the simple ratio and the normalized difference, was estimated for all WL bands combined along the observed reflectance spectrum. The highest h^2 estimates for both formats were obtained by combining WL bands of the red edge spectrum.

These new genetically driven pigment- and spectral reflectance- based markers (proxies of adaptive traits) may facilitate selection of stress resistant plant genotypes. Recent development of high-resolution spectral sensors carried by airborne and spaceborn devices make foliage spectral traits a viable technology for mass phenotyping in forest trees.

1. Introduction

Foliage content of photosynthetic pigments (chlorophylls and carotenoids) responds readily to environmental conditions; thus, it is frequently used as a stress indicator. Photosynthetic pigments are also the main biochemical compounds that determine the leaf optical properties (reflectance, transmittance and absorbance) in the visible region of the electromagnetic spectrum. Pigment contents can be estimated from reflectance spectra acquired by a spectroradiometer either in a laboratory (Croft et al., 2014) or by remote sensing techniques (Ustin and Gamon, 2010) using empirical methods or radiative transfer models. In several current studies reflectance indices are used as a proxy for pigment content without any training and validation of a particular index-pigment retrieval model on a corresponding reflectance and biochemistry dataset (Mõttus et al., 2014; Cavender-Bares et al., 2016; Flood et al., 2016). Airborne or spaceborne hyperspectral data provide information on larger spatial scales, which is advantageous in the case of forest stands.

At present, there is a limited knowledge on the genetic variability and control of photosynthetic pigment contents and spectral reflectance properties in forest trees. Thus, it is fundamental to decompose the observed variability of these indices into the underlying genetic and environmental factors and their respective interaction. Knowledge of pigment content and pigment-related spectral signatures narrow-sense

* Corresponding author.
E-mail address: cepl@fld.czu.cz (J. Čepl).

https://doi.org/10.1016/j.rse.2018.10.001
Received 30 January 2018; Received in revised form 13 September 2018; Accepted 1 October 2018
Available online 12 October 2018
0034-4257/

heritability (h^2) is critical to breeding programs, as these traits could be utilized as indirect proxies of desired phenotypes (e.g. to identify genotypes with drought-resistance, stress tolerance, etc.).

Relationship among the content of photosynthetic pigments, water status, other physiological features, and foliage spectral properties can be modeled by quantitative spectroscopic methods (e.g. Hernández-Clemente et al., 2012; Lhotáková et al., 2013). Needle characteristics derived from reflectance spectra (quantified by vegetation indices, e.g. the normalized difference vegetation index, NDVI) then approximate the physiological status of an individual tree or a population at a stand level (Campbell et al., 2004).

The red edge corresponds to a wavelength, which is defined mathematically as the inflection point position on the slope connecting the reflectance in the red and the NIR spectral regions (Horler et al., 1983). The red edge is very sensitive with regards to plant condition and it shifts to a shorter wavelength when the chlorophyll (Rock et al., 1988) or nitrogen (Mutanga and Skidmore, 2007) content decreases. Thus, the position of the red edge provides an indication of altered plant physiological condition due to air pollution (Campbell et al., 2004) or nutrient content (Mutanga and Skidmore, 2007). In a recent study, Feng et al. (2017) identified candidate genes controlling chlorophyll content in a thorough genome-wide association study of > 1500 hyperspectral indices in rice. They demonstrated that the red edge (680–760 nm) is vital to phenotypic and genetic insights into rice research.

Leaf spectra can also provide tools for elucidating genetic differences among populations. As shown by Cavender-Bares et al. (2016), full leaf spectral reflectance provides accurate models for differentiating among individual oak species within the genus or even different populations of a single oak species. Madritch et al. (2014) discriminated genotypic identity within the species of trembling aspen (*Populus tremuloides* Michx) using imaging spectroscopy and concluded that canopy spectra better described the genetic distance among genotypes than foliar traits. Spectral reflectance of dried and ground needles was used to distinguish various species of genus *Pinus* (Espinoza et al., 2012) and their hybrids (Meder et al., 2014). Thus, leaf spectral data appear to be relevant and have potential for high-throughput phenotyping approaches in forest tree breeding. Foliar spectral reflectance can be used as a predictor in phenomic selection, reducing high phenotyping and genotyping costs in breeding programs (Rincent et al., 2018).

As far as we know, no previous study has focused on spectral reflectance h^2 in conifers. Our study was based on two experimental plantations of Scots pine (*Pinus sylvestris* L.). Plantations were comprised of half-sib progenies of two seed orchards that were later converted into full-sib progenies through the marker-based pedigree reconstruction in accordance with the concept of Breeding Without Breeding (El-Kassaby et al., 2007; El-Kassaby and Lstibůrek, 2009). The reconstructed pedigree information facilitates conventional genetic evaluation (primarily estimation of h^2 and precision of additive genetic values). Progeny trials of forest trees are commonly used for evaluating production traits (such as height or volume), but they can also reveal information on traits indirectly influenced by environmental acclimation such as chlorophyll fluorescence (Čepl et al., 2016) or photosynthetic pigment content and spectral reflectance traits as shown in the current study.

The main aim of the present study was to investigate the existence and extent of heritable variation in needle spectral reflectance of Scots pine. Our method comprised of 1) the analysis of pigment- and water-related reflectance indices; 2) the assessment of biochemically determined contents of photosynthetic pigments and their ratios; 3) the gravimetrical estimation of water content in needles. The next aim of our study was to estimate h^2 in 1 nm wavelength bands along the wide range of the reflectance spectrum (400–2500 nm), which has not been previously published. Additionally, we explored the most widely used reflectance indices (normalized difference indices with special emphasis to NDVI and simple ratio indices) in terms of their heritable variation.

Table 1
Description of research sites.

Characteristics	Study sites	
	Skelná Huť	Nepomuk
Geographic coordinates	49°55′53.489″N, 13°6′43.268″E	49°29′40.735″N, 13°33′5.702″E
Altitude	610 m	490 m
Soil type	Planosol (PL)	Stagnosol (ST) Dystric Cambisol (CMdy)
LAI – hemisurface	5.2 (SE 0.1)	6.9 (SE 0.1)
Age of trees during measurement [years]	20	23
Approximate tree height [m][a]	12	14
Date of measurements	August 4–6, 2014	July 14–18, 2014
Number of measured trees	208	315

LAI – Leaf area index, SE – standard error.
[a] Last accurate measurement of height was conducted in 2007, giving 7.88 m (SD 1.59 m) and 10.02 m (SD 0.88 m) for Skelná Huť site and Nepomuk site, respectively.

2. Material and methods

2.1. Site description

The study was conducted on a Scots pine population originating from Western Bohemia, Czech Republic (Kaňák et al., 2009). Two sites were evaluated as being under no apparent environmental stress (for details see Čepl et al., 2016). Measurements were carried out on two half-sib progeny test plots planted as randomized incomplete block designs on two geographically distinct sites (Skelná Huť and Nepomuk) located in the western part of the Czech Republic (Western Bohemia; for specification, see Table 1). These test plots were grown from seeds originating from two separate seed orchards, each composed of selected plus-trees of Scots pine, all originating from the Western Bohemia provenance (Kaňák et al., 2009).

2.2. Sample collection and measurement setup

Sampling and measurements of needle reflectance, pigment and water content took place during the summer (July and August) of 2014 (Table 1). All trees included in our analysis possessed sun-exposed crowns and were previously genotyped (see section on Pedigree reconstruction). Only fully sun-exposed branches from the mid-to-upper part of a crown were cut using the combination of stepladder and telescopic pole-scissors generally from the southern crown side. However, as proven earlier, azimuth orientation of a branch does not play a role in variation of needle spectral, structural and biochemical parameters unless the branches are exposed to the full sunlight (Lhotáková et al., 2007). From each tree, a single branch was used for biochemical and spectral analyses: one sample for each analysis per branch was measured. In total 208 and 315 trees were sampled and processed biochemically and spectrally across the two test sites. Sampling was done on the two sites on three to four consecutive days from 10:00 am to 4:00 pm (Central European Summer Time). The length of collected branches was at least 100 cm to minimize desiccation; this was verified in a preliminary pilot experiment (Čepl et al., 2016). Branch stumps were wrapped in moistened towels and at the end of the day, they were transported to the laboratory to be processed the next day in the early morning. The collection time was recorded for each branch and the sample order was kept for spectral measurements so that all measurements were accomplished not later than 24 h after being cut. According to Richardson and Berlyn (2002), reflectance measurements in this setup are comparable to in-situ measurements.

Previous-year needles were selected, because the needles from the current season were not yet fully developed at the time of collection. This meant that reflectance measurements took place at the apical ends of sampled branches, with ample amount of wood tissue between the cut end and the measured needles, ensuring no embolism in the investigated branch section (Richardson and Berlyn, 2002).

2.3. Spectral measurements

Needle spectral reflectance information was obtained as a bidirectional reflectance factor (BRF) measured between 350 and 2500 nm using an ASD FieldSpec 4 Wide-Res portable spectroradiometer (ASD Inc., USA) attached to the fiber optic contact probe (ASD Plant Probe) with the circular field of view of 133 mm^2 (diameter 11 mm). The built-in halogen bulb, aligned at 12° to the probe body, was used as a light source. We assumed a bi-directional view-illumination geometry (Schaepman-Strub et al., 2006) as the contact probe illuminates the needles very close to their surface. The radiance spectra were normalized against a 99% Spectralon white reference to produce BRF for each measurement. Several shoots (3–5) from each single branch sampled from a tree were placed on a glass Petri dish coated with a matt black heat resistant paint (Peter Kwasny GmbH, Germany) resulting in spectrally black surface (background reflectance did not exceed 0.3%) to minimize the background spectral noise or radiation transmitted through the needles. The contact probe was placed on a continuous needle layer, and the full field of view of the contact probe was covered by the needles. The needle surface was illuminated by a constant light source inside the contact probe. A Scots pine needle surface is flat on one side and curved on the other, which could produce differences in adaxial and abaxial BRF at the needle level. Therefore, the needles were kept attached to the shoot and a random mixture of both needle sides was exposed to the contact probe. The scan average on the spectroradiometer was set to 15 to avoid foliage overheating (Eitel et al., 2006). The integration time of the spectroradiometer was set to 136 ms and the time necessary for scanning one contact probe field of view on a needle stack was not > 10 s. Needles were still attached to the twig during the spectra measurement. For each needle stack, five independent measurements were taken on different parts of the needle stack, and their medians (used as a measure of central tendency to exclude technical outliers) were calculated.

2.4. Spectral vegetation indices calculation

At the leaf level, empirical relationships between indices and leaf traits can be affected by leaf structure. We therefore selected vegetation indices that were previously developed or tested on needle-like leaves, ideally on *Pinus sylvestris* or other species from the *Pinaceae* family. For our study, we selected 30 vegetation indices (Table 2) frequently used for estimating photosynthetic pigment content, their ratios and water content from leaf spectra. The main three types of indices used were: 1) simple ratios (SR, calculated as ratio of reflectance in wavelengths x and y), 2) normalized difference indices (ND, calculated as ratio of reflectance differences in wavelengths x − y and sum of x + y) and their modified versions, and 3) derivative indices (e.g. $REIP_{derivative}$, D_{718}/D_{704}). The indices were selected according to the strength of the linear relationships with total chlorophyll or carotenoid contents, total carotenoid to total chlorophyll ratio (Car/Chl) and water content (as described in the studies cited in Table 2).

Coefficient of determination (R^2) was used as a goodness-of-fit between reflectance indices and pigments (Table 4).

2.5. Content of photosynthetic pigments and water in needles

Photosynthetic pigments (chlorophylls *a* and *b*, total carotenoids) were extracted in dark conditions, at 4 °C for seven days with *N,N*-dimethylformamide (Porra et al., 1989) and their contents were determined spectrophotometrically. Pigment concentrations were calculated according to the equations reported by Wellburn (1994) and expressed as the amount of the respective pigment per unit of dry matter (g/kg).

Water content was determined as the percentage of water weight relative to the fresh needle weight (the fraction of biomass reduction after drying). Fresh needles were weighed, oven-dried at 80 °C for 48 h until the weight was constant, then weighed again and water content was calculated.

2.6. Pedigree reconstruction

Pedigree reconstruction was conducted across both sites to identify paternal individuals (Čepl et al., 2016). Parentage analysis was carried out using 10 previously published microsatellite markers (for details see Čepl et al., 2016). Markers were selected according to their performance for this sample set (the level of polymorphism, the absence of nonspecific amplification and the low probability of null allele occurrence).

Allele frequency analysis and subsequent parentage assignment were carried out under a maximum likelihood framework implemented in CERVUS 3.0 (Kalinowski et al., 2007), which also accounts for genotyping errors and selfing.

The first scenario was paternal assignment with a known maternal parent (the half-sib progeny seed parent, partial pedigree reconstruction), then an alternative scenario with both parents assumed unknown was also evaluated (full pedigree reconstruction). The comparison of pedigree reconstruction under these two scenarios helped to reveal evident mismatches. Offspring individuals with no clear match to the recorded mother were excluded from the final set used in this study. To minimize experimental efforts, phenotypic pre-selection based on growth and stem straightness substantially reduced the number of fingerprinted individuals (Lstibůrek et al., 2011).

2.7. Statistical analyses and genetic parameter estimation

Pedigree-based genetic analysis was used under the assumptions of unrelated founders. Variance components and heritabilities were predicted by fitting the following univariate animal model (Henderson, 1984):

$$\boldsymbol{y} = \boldsymbol{X\beta} + \boldsymbol{Za} + \boldsymbol{e}$$

where $\boldsymbol{y}$ is the response matrix of phenotypic records for all the observed traits; $\boldsymbol{X}$ is the incidence matrix for the fixed effect $\boldsymbol{\beta}$ (intercept and site effect); $\boldsymbol{Z}$is the corresponding incidence matrix related to random additive genetic effects (breeding values, $\boldsymbol{a} \sim N(0, \boldsymbol{G})$; $\boldsymbol{G} = \sigma_a^2 \boldsymbol{A}$,product of the variance component explained by the tree effect and additive relationship matrix derived from the pedigree). The random residual error effects are normally and independently distributed as $\boldsymbol{e} \sim N(0, \boldsymbol{R})$; $\boldsymbol{R} = \boldsymbol{I}\sigma_e^2$ where $\boldsymbol{I}$ is the identity matrix and σ_e^2 is the residual variance.

Variance components estimates from the above model were used to estimate heritability ($h^2 = \sigma_a^2/\sigma_p^2$) of the measured traits, where σ_a^2 is the additive genetic variance and σ_p^2 is the total (phenotypic) variance. Standard error (SE) was calculated by the Δ approximation (Butler et al., 2007).

The model was analyzed using the ASReml-R software (Butler et al., 2007). Both sites were evaluated jointly to estimate heritabilities at the population level with an increased sample size (leading to a decreased SE of heritability and avoiding its bias). The Site factor was the only fixed effect in our model considering different site conditions and different ages occurring at both progeny test sites. As the original replicated design was not clearly visible in our dataset (due to the mortality), the common methods relying on x, y coordinates for modeling spatial variation could not be applied. Model inference was based on the asymptotic z-values for the random effects and approximated *F*-

Table 2
Details of selected spectral indices tested in this study. R^2 corresponds to the coefficient of determination published in the respective reference study. R stands for the BRF in the particular wavelength, D stands for the BRF curve first derivation value in the particular wavelength.

Index	Equation	Original reference
Chlorophyll indices from Croft et al. (2014) - *Picea mariana* Mill.; $R^2 > 0.55$		
Datt99	(R850 − R710) / (R850 − R680)	Datt (1999)
Macc01	(R780 − R710) / (R780 − R680)	Maccioni et al. (2001)
MNDVI8	(R755 − R730) / (R755 + R730)	Mutanga and Skidmore (2004)
NDVIre	(R750 − R705) / (R750 + R705)	Gitelson and Merzlyak (1994)
$REIP_{4\ point}$	$700 + 40\frac{(R670 + R780)/2 - R700}{R740 - R700}$	Guyot and Baret (1988)
$REIP_{derivative}$	Polynomial fitting	Pu et al. (2003)
VOG1	R740 / R720	Vogelmann et al. (1993)
ZM	R750 / R710	Zarco-Tejada et al. (2001)
Chlorophyll indices from Hernández-Clemente et al. (2012) - *Pinus sylvestris* L.; $R^2 \geq 0.80$		
$CI_{red\ edge}$	R750 / R710	Haboudane et al. (2002)
DattNIR-CabCar	R860 / R550 × R708	Datt (1998)
PSSRa	R800 / R680	Blackburn (1998)
TCARI/OSAVI	$\frac{3\left((R700 - R670) - 0.2\frac{(R700 - R550)}{(R700 / R670)}\right)}{1.16\,(R800 - R670) / (R800 + R670 + 0.16)}$	Haboudane et al. (2002)
Carotenoid: Chlorophyll indices from Hernández-Clemente et al. (2012) - *Pinus sylvestris* L.; $R^2 \geq 0.80$		
PRI	(R570 − R530) / (R570 + R530)	Gamon et al. (1992)
PSRI	R672 / (R550 + 3 × R708)	Merzlyak et al. (1999)
$SR_{530/570}$	R530 / R570	–
$SR_{540/560}$	R540 / R560	–
$SR_{540/570}$	R540 / R570	–
$SR_{550/560}$	R550 / R560	–
$SR_{550/570}$	R550 / R570	–
Carotenoid indices from Hernández-Clemente et al. (2012) - *Pinus sylvestris* L.; $R^2 \geq 0.80$		
CRI_{500}	1 / R515 − 1 / R550	Gitelson et al. (2003; 2006)
CRI_{700}	1 / R515 – 1 / R700	Gitelson et al. (2003; 2006)
PRIm1	(R515 − R530) / (R515 + R530)	Hernández-Clemente et al. (2012)
$SR_{515/560}$	R515 / R560	–
Water and chlorophyll indices from Stimson et al. (2005) - *Pinus edulis* Engelm.; $R^2 \geq 0.65$		
NDVI	(R860 − R690) / (R860 + R690)	Peñuelas et al. (1993)
NDWI	(R860 − R1240) / (R860 + R1240)	Gao (1996)
Chlorophyll and Carotenoid: Chlorophyll indices Mišurec et al. (2012, 2016) – *Picea abies* L. Karst		
TCARI	$3\left((R700 - R670) - 0.2\frac{(R700 - R550)}{(R700 / R670)}\right)$	Haboudane et al. (2002)
OSAVI	1.16 (R800 − R670)/(R800 + R670 + 0.16)	Rondeaux et al. (1996)
SIPI	(R800 − R445) / (R800 − R680)	Penuelas et al. (1995)
REP-LE	Red-edge position through linear extrapolation.	Cho and Skidmore (2006)
D_{718}/D_{704}	D718 / D704	Campbell et al. (2004)
MSR	$\frac{((R800 - R670) + 1)}{\sqrt{\left(\left(\frac{R800}{R670}\right) + 1\right)}}$	Chen (1996)

statistics for fixed effects. The significance of additive variance underlying heritability was evaluated by implementing a likelihood ratio test. In all cases, a significance level of 5% was considered. The methodology of model optimization and subsequent inference were based on Burgueño et al. (2000).

All calculations were performed in the R software environment, version 3.3.3 (R Core Team, 2017), and plots were made using ggplot2 (Wickham, 2009) and Plotly (Sievert et al., 2016) packages.

3. Results

3.1. Heritable variation in single wavelengths

Estimates of h^2 for 1 nm wavelength bands in the range of 400–2500 nm were plotted and revealed an interesting pattern (Fig. 1). Estimates of h^2 for reflectance in the VIS region of the electromagnetic spectrum were rather low and statistically non-significant, except for a part of the green spectral region (524–578 nm). It should be noted that h^2 estimates for all the wavelengths > 683 nm emerged as statistically significant. The highest h^2 estimate from the studied population ($\widehat{h}^2$~0.4) was found within a relatively narrow region, which peaked at a wavelength of 722 nm located in the red edge spectral region. Interestingly, this wavelength in the present study corresponded exactly to the position of the inflection point of steep reflectance rise in the red edge. h^2 estimates in both NIR (750–1400 nm) and SWIR (from 1400 nm) spectral regions were found to be noticeably higher in comparison to the VIS region, but they did not reach the maximum values detected in the red edge.

3.2. Revisiting simple ratio and normalized difference indices in terms of heritability

h^2 estimates of normalized differences for all wavelength combinations throughout the observed reflectance spectrum are presented in Fig. 2b. A detailed image is presented for the NDVI index family, generally formulated as normalized difference of near-infrared and red wavelength bands (NIR-RED/NIR + RED). We estimated h^2 of all combinations of RED (600–750 nm) and NIR (750–1400 nm) wavelengths, which revealed a clear trend, where the highest h^2 estimates were obtained by combining any NIR wavelength with WLs close to the red edge (see Fig. 2).

h^2 estimates of simple ratios for all wavelength combinations throughout the observed reflectance spectrum are presented in Fig. 2a. The results showed very similar pattern as in the case of normalized

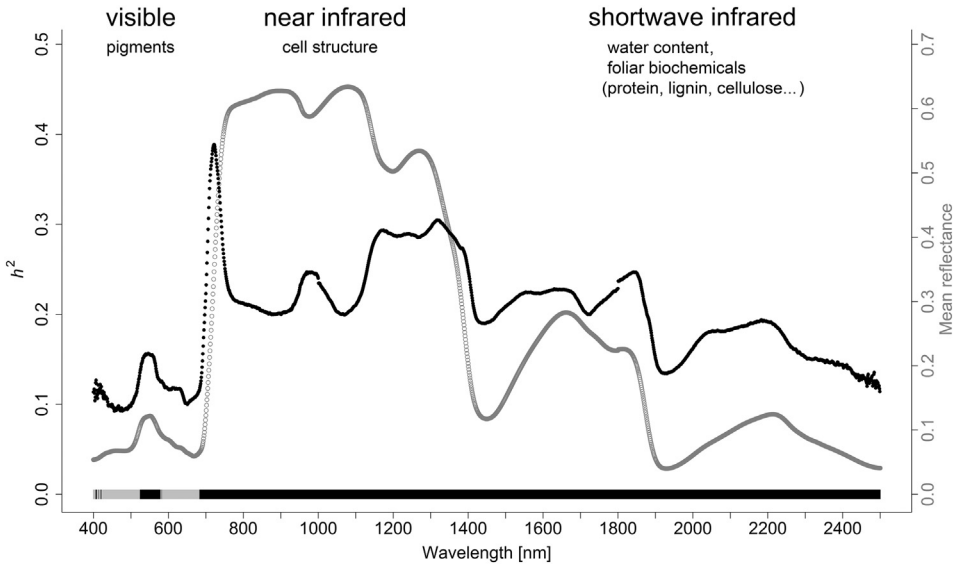

Fig. 1. Estimates of h^2 in 1 nm wavebands. Estimates of h^2 (right *y*-axis) for spectral reflectance at each wavelength are indicated by full black dots; region of significant h^2 at $\alpha = 0.05$ level is indicated by the black line on the *x*-axis; mean spectral reflectance for each wavelength from 400 nm to 2500 nm is indicated by grey circles, left *y*-axis. Main causal factors of foliar reflectance are indicated in the upper part of the plot.

differences.

3.3. Photosynthetic pigments, water content and reflectance indices: heritabilities and correlations

h^2 estimates of most widely used spectral reflectance indices (Table 2) averaged around 0.10, with values ranging from 0.02 to 0.22; here, the largest values of 0.21 and 0.22 were found for the red edge $REIP_{4\ point}$ index and the MNDVI8 index, respectively (Table 3).

Biochemically determined contents of pigments (chlorophylls *a* and *b*, total carotenoids) and gravimetrically assessed water content, together with calculated pigment ratios (Car/Chl $a + b$, Chl a/b) are displayed in Table 4 for each site separately.

The present study revealed that pigment and water contents were correlated with a variety of vegetation reflectance indices (see Table 2). Values of R^2 for the respective reflectance index and corresponding pigment content for each site are displayed in Table 5. Generally, R^2 values were rather low in the present study (maximum value of 0.4). h^2 estimates for these traits are displayed in Table 6. As apparent, water and pigment contents displayed negligible or non-significant h^2. In contrary, statistically significant h^2 in both pigment ratios of Chl a/b ($\widehat{h}^2 = 0.24$) and Car/Chl $a + b$ ($\widehat{h}^2 = 0.34$) was found.

Chl *a* – chlorophyll *a*, Chl *b* – chlorophyll *b*, Car – carotenoids, Car/Chl – ratio of total carotenoids to total chlorophyll $a + b$. Site effect describes the statistical differences between two sites; asterisks denote statistical significance ($^{***}P \leq 0.001$, ns = not significant). Number of trees analyzed at both sites: $N_{Skelná\ Huť} = 208$; $N_{Nepomuk} = 315$.

4. Discussion

Spectral signatures derived from foliar pigment content are frequently used as non-specific stress markers in forest trees (Pukacki and Kamińska-Rożek, 2005; Kopačková et al., 2014; Mišurec et al., 2016). Knowledge of any underlying genetic control would be highly beneficial for interpretations in many fields of basic and applied studies in plant ecophysiology, and forest genetics.

4.1. Heritability of needle spectral reflectance indices

Genetic variability of spectral traits in tree species has been rarely assessed and we are not aware of any study in conifers. For the strawberry tree (*Arbutus unedo* L.), h^2 of four spectral reflectance indices ($R750/R550$: $\widehat{h}^2 = 0.56$; NVDI: $\widehat{h}^2 = 0.96$; $R900 / R970$: $\widehat{h}^2 = 0.64$ and PRI: $\widehat{h}^2 = 0.80$) was investigated as an important proxy of adaptation in a changing climate (Santiso et al., 2015). Broad-sense heritability (H^2) estimates of three spectral indices (NDVI: $\widehat{H}^2 = 0.62$; VARI: $\widehat{H}^2 = 0.77$ and SRPI: $\widehat{H}^2 = 0.60$) derived from multispectral airborne data was acquired on apple trees (*Malus domestica* Borkh.) as reported by Virlet et al. (2015).

More data on heritability of leaf spectral reflectance have been acquired from herbaceous plants and crops. In winter wheat (*Triticum aestivum* L.), $\widehat{h}^2$ of vegetation indices ranged between 0.46 and 0.74, and $\widehat{h}^2$ of water indices ranged from 0.49 to 0.78 (Prasad et al., 2007). Flood et al. (2016) estimated H^2 in chlorophyll reflectance index $(R700^{-1} - R790^{-1}) \times R790$ for various genotypes of *Arabidopsis thaliana* (L.) Heynh. and they reported a value of $\widehat{H}^2 = 0.5$.

In comparison to these studies, our h^2 estimates for Scots pine are lower (0.02 to 0.22). However, our material was comprised of trees grown in natural conditions, thus encountering a more heterogeneous environment. As highlighted by Geber and Griffen (2003), heritability of various plant functional traits assessed in controlled environments with uniform progeny was often overestimated relative to the natural environment. Moreover, Virlet et al. (2015) reported heritability estimates based on clonal trial data, allowing for higher precision of heritability estimates.

4.2. Heritability in single wavelengths of needle spectral reflectance

Apart from the standard approach of the calculation of the respective spectral reflectance indices, the heritable variation of reflectance in narrow wavelength bands (1 nm) was investigated. We observed a visible pattern based on variable heritability detected along the reflectance curve.

In the VIS region of the spectrum, plants absorb blue and red light and utilize it for photosynthesis. $\widehat{h}^2$ for the reflectance spectral region between 400 and 524 nm (blue) and 578–683 nm (red) was not significant in this study. In contrast, rather low but significant $\widehat{h}^2$ for the green spectrum was detected. One possible explanation of the relatively lower h^2 in the VIS spectral region might be the stabilizing selective pressure on reflectance properties connected to photosynthesis - a phenomenon known as the Bulmer effect (Bulmer, 1971). However, this statement could be contradicted by the fact that pigment ratios displayed significantly moderate h^2. Another explanation of low h^2 might be due to additional reflectance variability caused by chloroplast movement inside mesophyll cells in response to light. Although this phenomenon was not documented in conifers, it was described in black

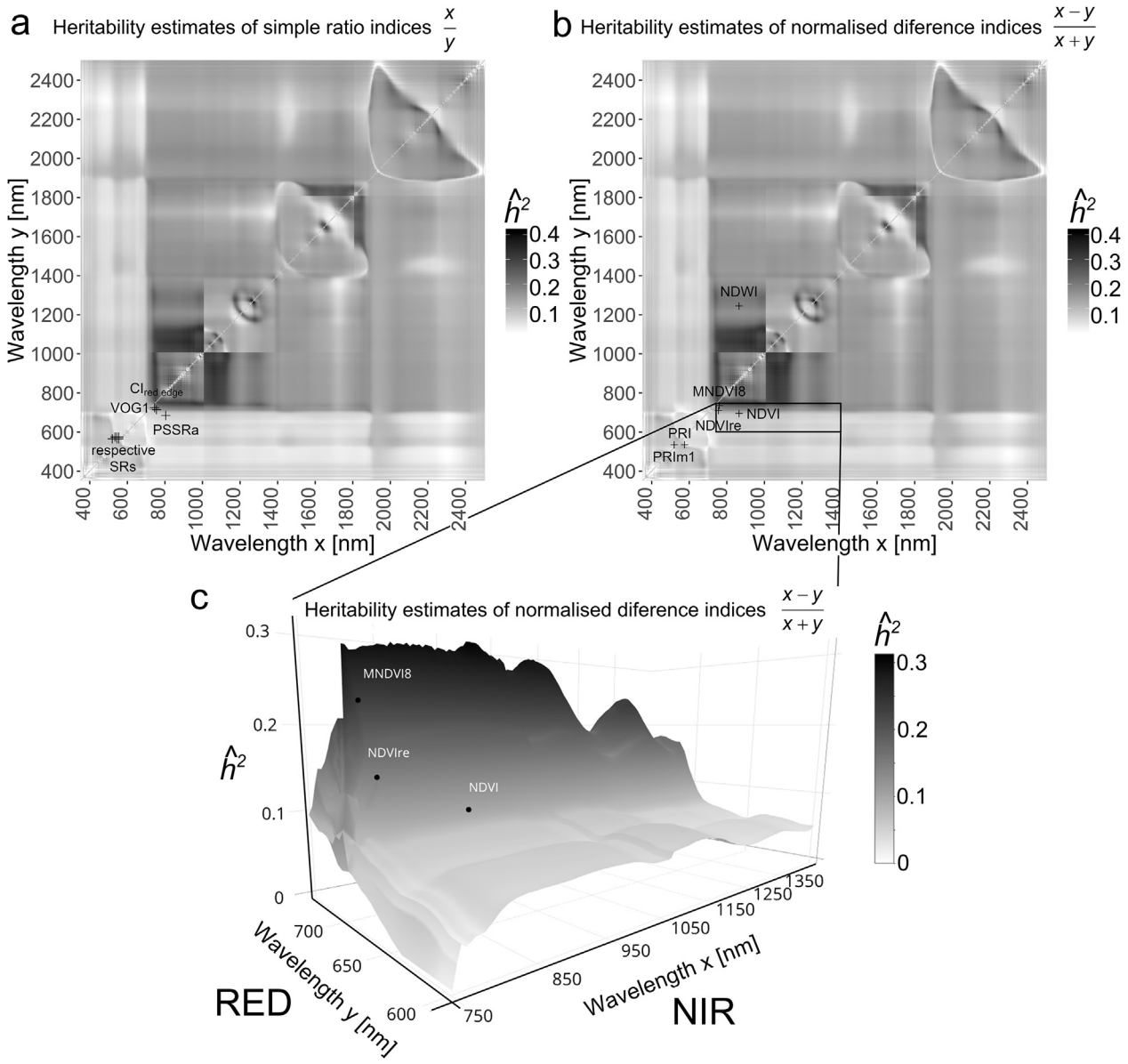

Fig. 2. Estimates of h^2 for simple ratio and normalized difference index formats. (a) all combinations of wavelength simple ratios with corresponding $\hat{h}^2$ pictured on the grey scale. Positions of chosen established simple ratio indices are indicated by black crosses. (b) all combinations of wavelength normalized difference indices with corresponding $\hat{h}^2$ pictured on the grey scale. Positions of chosen established normalized difference indices are indicated by black crosses. (c) all combinations of wavebands within a range typically used to calculate NDVI (x and y axis) with respective $\hat{h}^2$ (z axis).

cottonwood (*Populus trichocarpa*, Torr. & Gray) that chloroplast movement could decouple reflectance measurements from actual chlorophyll content as chloroplasts closer to the leaf adaxial surface may obscure those that are deeper in (Momayyezi and Guy, 2017).

The photon energy at wavelengths above 710 nm is not sufficient to synthesize organic molecules in higher plants. Plants, thus, reflect more light in NIR, starting with a sharp rise in reflectance in the spectral region called the red edge. In our scenario, the inflection point of the mean reflectance rise in the red edge is located at 722 nm. Interestingly, the apex of the narrow peak of h^2 ($\hat{h}^2$ = 0. 39; SE 0.13) can also be found at the wavelength of 722 nm, which exhibits the highest h^2 estimate in our study. A similar pattern of h^2 in VIS and red edge was observed also in maize based on the results presented in Obeidat (2017, Ph.D. thesis; graph on p. 150). However, the author in the accompanying text did not mention or discuss the pattern. Recently, h^2 of several red edge spectral indices, genetically and phenotypically correlated with chlorophyll content, was described in rice enhanced by candidate gene identification (Feng et al., 2017). Altogether, these findings suggest this trend to be more general, unrestricted to the species chosen, population and environmental conditions and open the potential for using hyperspectral red edge leaf traits as valuable markers for high-throughput, nondestructive phenotyping in plants.

In the NIR and SWIR regions, relatively high h^2 values with several broad peaks were detected. It should be noted that reflectance spectra contain even more complex information about a wide range of biochemical and structural needle parameters, such as lignin and cellulose contents (Fourty et al., 1996) or lignin and soluble phenolics (Soukupova et al., 2002). Therefore, reflectance in specific wavelengths may give information about needle compounds other than pigments and could be used as indirect selection markers. As discussed by Ollinger (2011), we can often gain more insight about the functioning of plants by examining wavelengths that are not used in photosynthesis than by examining those that are.

Additionally, based on the findings in h^2 data of single wavelengths,

Table 3
Heritability of tested reflectance indices.

Index	$\hat{h}^2$	SE	Significance
MNDVI8	0.22	0.09	*
Datt99	0.17	0.07	*
Macc01	0.17	0.07	*
VOG1	0.14	0.07	*
ZM	0.15	0.08	*
NDVIre	0.14	0.07	*
PSSRa	0.06	0.05	ns
$CI_{red\ edge}$	0.15	0.08	*
PSSRb	0.05	0.05	ns
DattNIR-CabCar	0.18	0.09	*
TCARI/OSAVI	0.16	0.08	*
$SR_{550/570}$	0.03	0.04	ns
PSRI	0.07	0.05	*
$SR_{540/570}$	0.02	0.04	ns
$SR_{550/560}$	0.07	0.06	ns
PRI	0.04	0.05	ns
$SR_{530/570}$	0.04	0.05	ns
$SR_{540/560}$	0.09	0.06	*
$SR_{515/560}$	0.10	0.06	*
PRIm1	0.08	0.06	*
CRI500	0.07	0.06	ns
CRI700	0.04	0.05	ns
NDWI	0.18	0.08	*
NDVI	0.10	0.06	*
$REIP_{derivative}$	0.18	0.08	*
$REIP_{4\ point}$	0.21	0.08	*

SE – standard error.
* Significance at $\alpha = 0.05$ level.

Table 5
Needle pigment contents and ratios in dry matter [$g \times kg^{-1}$] and foliar water content.

Trait	Nepomuk		Skelná Huť		Site effect
	Mean	SD	Mean	SD	
Chl *a*	3.39	0.58	2.67	0.49	***
Chl *b*	1.18	0.25	0.90	0.19	***
Car	0.63	0.11	0.49	0.09	***
Chl *a* + *b*	4.57	0.82	3.57	0.67	***
Chl *a*/*b*	2.90	0.22	3.00	0.27	***
Car/Chl	0.14	0.01	0.14	0.01	ns
Water content	0.54	0.04	0.57	0.02	***

Table 6
Heritability of measured traits.

Trait	$\hat{h}^2$	SE	Significance
Chl *a*	0.07	0.05	*
Chl *b*	0.05	0.05	ns
Car	0.09	0.05	*
Chl *a* + *b*	0.06	0.05	ns
Chl *a*/*b*	0.24	0.08	*
Car/Chl	0.34	0.10	*
Water content	0.07	0.06	ns

Chl *a* – chlorophyll *a*, Chl *b* – chlorophyll *b*, Car – carotenoids, Car/Chl – ratio of total carotenoids to total chlorophyll *a* + *b*, SE – standard error.
* Significance at $\alpha = 0.05$ level.

Table 4
Coefficient of determination (R^2) as a measure of correlation among photosynthetic pigments and reflectance indices.

Site	Nepomuk							Skelná Huť						
Index	WC	Chl *a*	Chl *b*	Car	Chl *a* + *b*	Chl *a*/*b*	Car/Chl	WC	Chl *a*	Chl *b*	Car	Chl *a* + *b*	Chl *a*/*b*	Car/Chl
MNDVI8	NA	0.32	0.25	NA	0.31	0	NA	NA	0.24	0.25	NA	0.25	0.08	NA
Datt99	NA	0.31	0.25	NA	0.30	0	NA	NA	0.32	0.33	NA	0.33	0.11	NA
Macc01	NA	0.31	0.25	NA	0.30	0	NA	NA	0.31	0.33	NA	0.33	0.11	NA
VOG1	NA	0.33	0.25	NA	0.32	0	NA	NA	0.24	0.26	NA	0.25	0.11	NA
ZM	NA	0.34	0.26	NA	0.33	0	NA	NA	0.25	0.28	NA	0.27	0.11	NA
NDVIre	NA	0.34	0.27	NA	0.33	0	NA	NA	0.23	0.26	NA	0.25	0.11	NA
PSSRa	NA	0.12	0.08	NA	0.11	0	NA	NA	0.01	0.01	NA	0.01	0.01	NA
$CI_{red\ edge}$	NA	0.34	0.26	NA	0.33	0	NA	NA	0.25	0.28	NA	0.27	0.11	NA
PSSRb	NA	0.21	0.18	NA	0.21	0	NA	NA	0.07	0.09	NA	0.08	0.06	NA
DattNIR_CabCar	NA	0.26	0.21	0.32	0.26	0	NA	NA	0.24	0.27	0.21	0.26	0.11	NA
TCARI_OSAVI	NA	0.33	0.26	0.36	0.32	0	NA	NA	0.37	0.40	0.32	0.39	0.15	NA
$REIP_{derivative}$	NA	0.27	0.23	NA	0.27	NA	NA	NA	0.21	0.22	NA	0.22	NA	NA
$REIP_{4\ point}$	NA	0.32	0.28	NA	0.32	NA	NA	NA	0.36	0.35	NA	0.36	NA	NA
TCARI	NA	0.29	0.23	0.32	0.28	NA	NA	NA	0.37	0.40	0.33	0.39	NA	NA
SIPI	NA	0.01	0.03	0.01	0.02	0.05	0.02	NA	0.01	0.02	0.01	0.01	0.03	0.01
REP_LI	NA	0.30	0.24	0.30	0.30	0	NA	NA	0.30	0.30	0.25	0.31	0.08	NA
OSAVI	NA	0.10	0.08	NA	0.10	NA	NA	NA	0	0.01	NA	0	NA	NA
MSR	NA	0.11	0.07	0.15	0.10	0	0.02	NA	0.01	0.01	0.01	0.01	0.01	0
$SR_{550/570}$	NA	NA	NA	NA	NA	0	0	NA	NA	NA	NA	NA	0.01	0
PSRI	NA	NA	NA	NA	NA	0.01	0.01	NA	NA	NA	NA	NA	0.01	0.01
$SR_{540/570}$	NA	NA	NA	NA	NA	0	0	NA	NA	NA	NA	NA	0.02	0.02
$SR_{550/560}$	NA	NA	NA	NA	NA	0	0	NA	NA	NA	NA	NA	0	0
PM	NA	NA	NA	NA	NA	0	0	NA	NA	NA	NA	NA	0.03	0.04
$SR_{530/570}$	NA	NA	NA	NA	NA	0	0	NA	NA	NA	NA	NA	0.03	0.04
$SR_{540/560}$	NA	NA	NA	NA	NA	0.01	0	NA	NA	NA	NA	NA	0.03	0.04
$SR_{515/560}$	NA	NA	NA	NA	NA	0	0	NA	NA	NA	NA	NA	0.01	0.02
PRIml	NA	NA	NA	0	NA	NA	NA	NA	NA	NA	0.04	NA	NA	NA
CRI500	NA	NA	NA	0.13	NA	NA	NA	NA	NA	NA	0.01	NA	NA	NA
CRI700	NA	NA	NA	0.12	NA	NA	NA	NA	NA	NA	0.04	NA	NA	NA
NDWI	0.08	NA	NA	NA	NA	NA	NA	0	NA	NA	NA	NA	NA	NA
NDVI	0.10	0.03	0.03	0.02	0.03	0.02	0.01	0	0.19	0.18	0.21	0.02	0.19	0

WC – water content, Chl *a* – chlorophyll *a*, Chl *b* - chlorophyll *b*, Car – carotenoids, Car/Chl – ratio of total carotenoids to total chlorophyll *a* + *b*. NA – correlation not relevant for a given index.

we examined two widely used reflectance index formats – simple ratio and normalized difference. The patterns of h^2 estimates are similar for both index types with lower values for VIS combinations and higher values for red edge, NIR and SWIR combinations. An apparent break at 1000 nm might be attributed to the change of a measuring sensor in the spectroradiometer ASD FieldSpec 4 at this given wavelength. Interestingly, this break is not apparent in single wavelength h^2.

The index NDVI, defined as normalized difference between NIR and red spectrum (NIR − RED / NIR + RED), is broadly used to examine plant health and level of environmental stress over large areas from airborne or spaceborne devices. This index is often acquired by broad-band (50–100 nm bands) multispectral sensors, but the use of narrow-band sensors was proven to provide more sensitive measurements of specific plant variables (Hansen and Schjoerring, 2003; Marshall et al., 2016). Here we presented a thorough exploration of NDVI index in terms of h^2. Within all commonly applied combinations of spectral ranges in RED (600–750 nm) and NIR (750–1400 nm), h^2 estimates reached up to 0.34. Generally speaking, indices with high h^2 are more reliable markers of underlying plant fitness.

4.3. Heritability of pigment content and ratios

The studied Scots pine population exhibited rather low (0.05–0.09) or non-significant h^2 estimates in foliage water content and photosynthetic pigment content. Water content varies dramatically throughout the course of a day and transpiration rates change with the weather (wind, temperature, light), thus, the environmental effect probably prevails over genetics.

For pigment content, comparable results were published by García-Verdugo et al. (2010) for olive trees (*Olea europaea* subsp. *guanchica*), where almost zero h^2 was found for pigment traits. These authors suggested that the lack of h^2 might be due to the high phenotypic plasticity or strong patterns of selection in Mediterranean environments (García-Verdugo et al., 2010). Such a selection pattern might have occurred in our study due to the strong phenotypic pre-selection of the sampled trees aimed at “superior” genotypes based on profitable forestry traits.

On the other hand, both commonly reported pigment ratios displayed statistically significant, moderate h^2 (Chl a/b $\widehat{h}^2 = 0.24$; Car/Chl $a + b$ $\widehat{h}^2 = 0.34$). This finding may indicate that ratios could be associated with unique genetic architecture in comparison to single factor indices. This may also suggests that pigment ratios might be more sensitive indicators for some plant conditions than pigment contents solely. Additionally, phenology of these pigment ratios in conifers revealed their seasonal variability (Wong and Gamon, 2015; Gamon et al., 2016). Variation in phenology is known to have a strong genetic component and recently this was confirmed by genome wide association studies in forest trees (e.g. McKown et al., 2018).

4.4. Relation of needle spectral reflectance indices and pigment contents

In our study, we utilized reflectance indices that were reported to show high coefficients of determination (R^2) with respective pigment content or ratios on conifers in past studies (Table 2). Our analysis found low (maximum value of 0.4) values of R^2 for all studied index-pigment pairs (Table 4). These weak correlations among pigment contents, their ratios and water content may be caused by coniferous needle morphology in combination with contact probe measurement setup. Measurement setup can remarkably affect the leaf spectral signatures for planar leaves (Neuwirthová et al., 2017). For example, systematic overestimation of leaf reflectance is reported when measured by contact setup versus by integrating sphere (Hovi et al., 2017). The difference between contact probe and integrating sphere measurements are enhanced for coniferous needles (Potůčková et al., 2016). Multiple, multidirectional scattering between the needle layers and noise caused by woody parts of the twig may decouple the relation between needle reflectance and biochemistry. To avoid this effect, Einzmann et al. (2014) recommended measurement with a contact probe on needles detached from the shoot to gain pure needle spectra. Alternatively, special leaf clip with a small field of view, suitable for all types of leaves including needles (Gamon and Surfus, 1999) could be used to reduce both the measurement time and the effect of multiple scattering. According to Hovi et al. (2018), contact measurements are six times faster than those conducted with a single integrating sphere. As we measured a large number of samples (over 500), the faster contact measurement setup was chosen. Moreover, when dealing with conifers, needles have to be arranged in special sample holders, which is time consuming and requires further spectral preprocessing procedures (reviewed by Rautiainen et al., 2018). The needle morphology and anatomical structure can also play a role in correlation between spectral indices. Marín et al. (2016) stressed that the variability in coniferous needle reflectance spectra between 280 and 880 nm is primarily affected by needle structural traits (such as cuticle and needle thickness or mesophyll width) and to a lesser extent by needle biochemistry. Moreover, irradiation affects needle shape causing sun-exposed needles to be thicker than their shaded counterparts. This acts not only on macroscale in a crown vertical gradient, but also on microscale over a shoot corresponding to spatial orientation of individual needles on a shoot, as we reported recently (Kubínová et al., 2018). Thus, when measurements are made on needles attached to twigs to avoid desiccation, the circular needle arrangement on a shoot affects foliage reflectance. Consequently, the contribution of needle spatial arrangement on a shoot and the difference in needle morphology affected by an irradiance microgradient on the shoot to the foliage reflectance could have negatively influenced the strength of the correlation between the needle biochemical traits and reflectance indices.

Remotely sensed canopy-scale reflectance is affected by additional factors that may contribute to decoupling the relationship among biophysical traits and reflectance indices. These factors include needle clumping, needle and shoot angle distribution, presence of non-photosynthetic structures (branches and twigs), and soil/understory reflectance background (Homolová et al., 2013; Cavender-Bares et al., 2017; Rautiainen et al., 2018). In addition, remote sensing information could integrate several individuals, including signals originating from different species. Thus, proper separation of all contributing signals becomes essential (Yamasaki et al., 2017).

The upscaling from leaf level contact measurements to the canopy level is crucial to validate that the genetic variability of red edge spectral markers could be detected in remotely sensed canopy optical properties. Prospective results were shown by Madritch et al. (2014), who successfully mapped genetic variation among genets of trembling aspen in reflectance signatures at the canopy level. Further, based on laboratory spectral measurements, Kozhoridze et al. (2016) developed several indices able to distinguish genera and families of various plants in the Mediterranean forest using EO1 Hyperion images.

5. Conclusion

The existence of statistically significant heritable variation in spectral reflectance in Scots pine at different wavelengths was confirmed. The novelty of this study lies within the estimation of h^2 in 1 nm wavelength bands along the wide range of the reflectance spectrum (400–2500 nm). The highest h^2 estimate ($\widehat{h}^2 = 0.39$; SE 0.13) was detected for the waveband in 722 nm, corresponding to the red edge inflection point. Relatively high h^2 was found also in NIR and SWIR spectral regions. In contrast, all h^2 estimates of reflectance in VIS (except for the segment of the green spectrum region) were close to zero with no statistical significance.

The maximum h^2 detected at the red edge inflection point sheds new light on biological importance of this one-wavelength spectral feature.

The red edge not only provides an indication of the overall plant physiological condition, but also has considerable h^2 variation. Based on recent studies, it appears that the h^2 peak observed in the red edge inflection point could be a much more general phenomenon, and that this pattern of h^2 could be observed in a wide range of plant species not only specific populations and environments.

In this study, we showed that the variation in reflectance indices may be partially genetically driven. Knowledge about genetically driven pigment- or spectral reflectance- based stress markers may help to recognize genotypes resistant to abiotic stress. Moreover, the spectral signals, such as single wavelength reflectance or spectral indices, may be used as indirect markers for particular foliar parameters correlated to production or adaptive traits. This could have further implications for the use of hyperspectral data in vegetation observation and analysis.

Appropriate upscaling of leaf level contact measurements to the canopy level is necessary before genetically driven spectral markers from remotely acquired optical properties can be used for high-throughput phenotyping of trees on a large spatial scale.

Acknowledgement

We thank Lena Hunt for final language correction.

Funding

Internal Grant Agency of the Czech University of Life Sciences Prague CIGA, grant no. 20164306; National Agency for Agriculture Research (NAZV; Grant QJ1620110 and QJ1320013); “EXTEMIT - K”, No. CZ.02.1.01/0.0/0.0/15_003/0000433 financed by Operational Program Research. The NPUI project of the Ministry of Education, Youth and Sports of the Czech Republic (grant no. LO1417), the internal project of Charles University – SVV.

Author contributions

J.A. and M.L. formulated initial design of the research, J.Č., J.S., I.T. and J.K. collected plant material in a field campaign and Z.L., D.H., M.P., M.K. and O.R. processed samples in a laboratory. Subsequent data analysis was performed by S.G., J.S., J.K., I.T., J.H., A.K. and J.Č. and interpreted mainly by J.Č., J.S., Z.L., R.W., J.A. and M.L. Final writing of the manuscript was performed by J.Č., J.S., D.H., Z.L., A.K., R.W., S.G. and J.A.

References

Blackburn, G.A., 1998. Quantifying chlorophylls and carotenoids at leaf and canopy scales: An evaluation of some hyperspectral approaches. Remote Sens. Environ. 66, 273–285.
Bulmer, M., 1971. The effect of selection on genetic variability. Am. Nat. 105, 201–211.
Burgueño, J., Cadena, A., Crossa, J., Banziger, M., Gilmour, A.R., Cullis, B., 2000. User's Guide for Spatial Analysis of Field Variety Trials Using ASREML. Cimmyt.
Butler, D., Cullis, B.R., Gilmour, A.R., Gogel, B.J., 2007. ASReml-R Reference Manual. AsReml-R Estimates Variance Components Under a General Linear Mixed Model by Residual Maximum Likelihood (REML). State Queensland, Dep Prim Ind Fish, Brisbane, Queensland, Aust.
Campbell, P.K.E., Rock, B.N., Martin, M.E., Neefus, C.D., Irons, J.R., Middleton, E.M., Albrechtova, J., 2004. Detection of initial damage in Norway spruce canopies using hyperspectral airborne data. Int. J. Remote Sens. 25, 5557–5584.
Cavender-Bares, J., Meireles, J.E., Couture, J.J., Kaproth, M.A., Kingdon, C.C., Singh, A., Serbin, S.P., Center, A., Zuniga, E., Pilz, G., 2016. Associations of leaf spectra with genetic and phylogenetic variation in oaks: prospects for remote detection of biodiversity. Remote Sens. 8, 221.
Cavender-Bares, J., Gamon, J.A., Hobbie, S.E., Madritch, M.D., Meireles, J.E., Schweiger, A.K., Townsend, P.A., 2017. Harnessing plant spectra to integrate the biodiversity sciences across biological and spatial scales. Am. J. Bot. 104, 966–969.
Čepl, J., Holá, D., Stejskal, J., Korecký, J., Kočová, M., Lhoták̀ová, Z., Tomášková, I., Palovská, M., Rothová, O., Whetten, R.W., 2016. Genetic variability and heritability of chlorophyll a fluorescence parameters in Scots pine (*Pinus sylvestris* L.). Tree Physiol. 36, 883–895.
Chen, J.M., 1996. Evaluation of vegetation indices and a modified simple ratio for boreal applications. Can. J. Remote. Sens. 22, 229–242.
Cho, M.A., Skidmore, A.K., 2006. A new technique for extracting the red edge position from hyperspectral data: The linear extrapolation method. Remote Sens. Environ. 101, 181–193.
Croft, H., Chen, J.M., Zhang, Y., 2014. The applicability of empirical vegetation indices for determining leaf chlorophyll content over different leaf and canopy structures. Ecol. Complex. 17, 119–130.
Datt, B., 1998. Remote sensing of chlorophyll a, chlorophyll b, chlorophyll a + b, and total carotenoid content in Eucalyptus leaves. Remote Sens. Environ. 66, 111–121.
Datt, B., 1999. Visible/near infrared reflectance and chlorophyll content in Eucalyptus leaves. Int. J. Remote Sens. 20, 2741–2759.
Einzmann, K., Ng, W.T., Immitzer, M., Bachmann, M., Pinnel, N., Atzberger, C., 2014. Method analysis for collecting and processing in-situ hyperspectral needle reflectance data for monitoring Norway spruce. Photogramm. Eng. Remote. Sens. 2014, 423–434.
Eitel, J.U.H., Gessler, P.E., Smith, A.M.S., Robberecht, R., 2006. Suitability of existing and novel spectral indices to remotely detect water stress in *Populus* spp. For. Ecol. Manag. 229, 170–182.
El-Kassaby, Y.A., Lstibůrek, M., 2009. Breeding without breeding. Genet. Res. 91, 111–120.
El-Kassaby, Y.A., Lstibůrek, M., Liewlaksaneeyanawin, C., Slavov, G.T., Howe, G.T., 2007. Breeding Without Breeding: Approach, Example, and Proof of Concept. Proceedings of the IUFRO Division 2 Joint Conference: Low Input Breeding and Conservation of Forest Genetic Resources. Antalya, Turkeypp. 43–54.
Espinoza, J.A., Hodge, G.R., Dvorak, W.S., 2012. The potential use of near infrared spectroscopy to discriminate between different pine species and their hybrids. J. Near Infrared Spectrosc. 20 (4), 437–447.
Feng, H., Guo, Z., Yang, W., Huang, C., Chen, G., Fang, W., Xiong, X., Zhang, H., Wang, G., Xiong, L., Liu, Q., 2017 Jun 30. An integrated hyperspectral imaging and genome-wide association analysis platform provides spectral and genetic insights into the natural variation in rice. Sci. Rep. 7 (1), 4401.
Flood, P.J., Kruijer, W., Schnabel, S.K., Schoor, R., Jalink, H., Snel, J.F.H., Harbinson, J., Aarts, M.G.M., 2016. Phenomics for photosynthesis, growth and reflectance in Arabidopsis thaliana reveals circadian and long-term fluctuations in heritability. Plant Methods 12, 14.
Fourty, T., Baret, F., Jacquemoud, S., Schmuck, G., Verdebout, J., 1996. Leaf optical properties with explicit description of its biochemical composition: direct and inverse problems. Remote Sens. Environ. 56, 104–117.
Gamon, J.A., Surfus, J.S., 1999. Assessing leaf pigment content and activity with a reflectometer. New Phytol. 143, 105–117.
Gamon, J.A., Peñuelas, J., Field, C.B., 1992. A narrow-wave band spectral index that tracks diurnal changes in photosynthetic efficiency. Remote Sens. Environ. 41, 35–44.
Gamon, J.A., Huemmrich, K.F., Wong, C.Y., Ensminger, I., Garrity, S., Hollinger, D.Y., Noormets A Peñuelas, J., 2016. A remotely sensed pigment index reveals photosynthetic phenology in evergreen conifers. Proc. Natl. Acad. Sci. U. S. A. 113, 13087–13092.
Gao, B.C., 1996. NDWI—A normalized difference water index for remote sensing of vegetation liquid water from space. Remote Sens. Environ. 58, 257–266.
García-Verdugo, C., Méndez, M., Velázquez-Rosas, N., Balaguer, L., 2010. Contrasting patterns of morphological and physiological differentiation across insular environments: phenotypic variation and heritability of light-related traits in Olea europaea. Oecologia 164, 647–655.
Geber, M.A., Griffen, L.R., 2003. Inheritance and natural selection on functional traits. Int. J. Plant Sci. 164, S21–S42.
Gitelson, A.A., Merzlyak, M.N., 1994. Quantitative estimation of chlorophyll-a using reflectance spectra: experiments with autumn chestnut and maple leaves. J. Photochem. Photobiol. B 22, 247–252.
Gitelson, A.A., Gritz, U., Merzlyak, M.N., 2003. Relationships between leaf chlorophyll content and spectral reflectance and algorithms for non-destructive chlorophyll assessment in higher plant leaves. Plant Physiol. 160, 271–282.
Gitelson, A.A., Keydan, G.P., Merzlyak, M.N., 2006. Three-band model for noninvasive estimation of chlorophyll, carotenoids, and anthocyanin content in higher plant leaves. Geophys. Res. Lett. 33.
Guyot, G., Baret, F., 1988. Utilisation de la Haute Resolution Spectrale Pour Suivre l'etat des Couverts Vegetaux. In: Proceedings, 4th international colloquium “Spectral Signatures of Objects in Remote Sensing”, Aussois, January 1988, 18–2, ESA, ESA Publication SP-287, Paris, pp. 279–286.
Haboudane, D., Miller, J.R., Tremblay, N., Zarco-Tejada, P.J., Dextraze, L., 2002. Integrated narrow-band vegetation indices for prediction of crop chlorophyll content for application to precision agriculture. Remote Sens. Environ. 81, 416–426.
Hansen, P.M., Schjoerring, J.K., 2003. Reflectance measurement of canopy biomass and nitrogen status in wheat crops using normalized difference vegetation indices and partial least squares regression. Remote Sens. Environ. 86, 542–553.
Henderson, C.R., 1984. Application of Linear Models in Animal Breeding. University of Guelph.
Hernández-Clemente, R., Navarro-Cerrillo, R.M., Zarco-Tejada, P.J., 2012. Carotenoid content estimation in a heterogeneous conifer forest using narrow-band indices and PROSPECT+ DART simulations. Remote Sens. Environ. 127, 298–315.
Homolová, L., Malenovský, Z., Clevers, J.G.P.W., García-Santos, G., Schaepman, M.E., 2013. Review of optical-based remote sensing for plant trait mapping. Ecol. Complex. 15, 1–16.
Horler, D.N.H., Dockray, M., Barber, J., Barringer, A.R., 1983. Red edge measurements for remotely sensing plant chlorophyll content. Adv. Space Res. 3, 273–277.
Hovi, A., Raitio, P., Rautiainen, M., 2017. A spectral analysis of 25 boreal tree species. Silva Fenn. 51, 1–16.
Kalinowski, S.T., Taper, M.L., Marshall, T.C., 2007. Revising how the computer program CERVUS accommodates genotyping error increases success in paternity assignment.

Mol. Ecol. 16, 1099–1106.
Kaňák, J., Klápšte, J., Lstibůrek, M., 2009. Initial evaluation of seed orchards of scots pine in the western Czech republic. Zpravy Lesn Vyzk 189–204.
Kopačková, V., Mišurec, J., Lhotáková, Z., Oulehle, F., Albrechtová, J., 2014. Using multi-date high spectral resolution data to assess the physiological status of macro-scopically undamaged foliage on a regional scale. Int. J. Appl. Earth Obs. Geoinf. 27, 169–186.
Kozhoridze, G., Orlovsky, N., Orlovsky, L., Blumberg, D.G., Golan-Goldhirsh, A., 2016. Remote sensing models of structure-related biochemicals and pigments for classifi-cation of trees. Remote Sens. Environ. 186, 184–195.
Kubínová, Z., Janáček, J., Lhotáková, Z., Šprtová, M., Kubínová, L., Albrechtová, J., 2018. Norway spruce needle size and cross section shape variability induced by irradiance on a macro-and microscale and CO_2 concentration. Trees 32, 231–244.
Lhotáková, Z., Albrechtová, J., Malenovský, Z., Rock, B.N., Polák, T., Cudlín, P., 2007. Does the azimuth orientation of Norway spruce (*Picea abies* L. Karst.) branches within sunlit crown part influence the heterogeneity of biochemical, structural and spectral characteristics of needles? Environ. Exp. Bot. 59, 283–292.
Lhotáková, Z., Brodský, L., Kupková, L., Kopačková, V., Potůčková, M., Mišurec, J., Klement, A., Kovářová, M., Albrechtová, J., 2013. Detection of multiple stresses in Scots pine growing at post-mining sites using visible to near-infrared spectroscopy. Environ. Sci.: Processes Impacts 15, 2004–2015.
Lstibůrek, M., Ivanková, K., Kadlec, J., et al., 2011. Breeding without breeding: minimum fingerprinting effort with respect to the effective population size. Tree Genet. Genomes 7, 1069–1078.
Maccioni, A., Agati, G., Mazzinghi, P., 2001. New vegetation indices for remote mea-surement of chlorophylls based on leaf directional reflectance spectra. J. Photochem. Photobiol. B 61, 52–61.
Madritch, M.D., Kingdon, C.C., Singh, A., Mock, K.E., Lindroth, R.L., Townsend, P.A., 2014. Imaging spectroscopy links aspen genotype with below-ground processes at landscape scales. Philos. Trans. R. Soc. Lond. Ser. B Biol. Sci. 369, 20130194.
Marín, S.D.T., Novák, M., Klančnik, K., Gaberščik, A., 2016. Spectral signatures of conifer needles mainly depend on their physical traits. Pol. J. Ecol. 64, 1–13.
Marshall, M., Thenkabail, P., Biggs, T., Post, K., 2016. Hyperspectral narrowband and multispectral broadband indices for remote sensing of crop evapotranspiration and its components (transpiration and soil evaporation). Agric. For. Meteorol. 218, 122–134.
McKown, A.D., Klápště, J., Guy, R.D., El-Kassaby, Y.A., Mansfield, S.D., 2018. Ecological genomics of variation in bud-break phenology and mechanisms of response to climate warming in *Populus trichocarpa*. New Phytol. 220, 300–316.
Meder, R., Kain, D., Ebdon, N., Macdonell, P., Brawner, J.T., 2014. Identifying hy-bridisation in *Pinus* species using near infrared spectroscopy of foliage. J. Near Infrared Spectrosc. 22 (5), 337–345.
Merzlyak, M.N., Gitelson, A.A., Chivkunova, O.B., Rakitin, V.Y., 1999. Non-destructive optical detection of leaf senescence and fruit ripening. Physiol. Plant. 106, 135–141.
Mišurec, J., Kopacková, V., Lhotáková, Z., Albrechtova, J., Hanus, J., Weyermann, J., Entcheva-Campbell, P., 2012. Utilization of hyperspectral image optical indices to assess the Norway spruce forest health status. J. Appl. Remote Sens. 6, 063545.
Mišurec, J., Kopačková, V., Lhotáková, Z., Campbell, P., Albrechtová, J., 2016. Detection of spatio-temporal changes of Norway spruce forest stands in ore mountains using Landsat time series and airborne hyperspectral imagery. Remote Sens. 8, 92.
Momayyezi, M., Guy, R.D., 2017. Blue light differentially represses mesophyll con-ductance in high vs low latitude genotypes of *Populus trichocarpa* Torr. & Gray. J. Plant Physiol. 213, 122–128.
Mõttus, M., Sulev, M., Hallik, L., 2014. Seasonal course of the spectral properties of alder and birch leaves. IEEE J. Sel. Top. Appl. Earth Obs. Remote Sens. 7, 2496–2505.
Mutanga, O., Skidmore, A.K., 2004. Narrow band vegetation indices overcome the sa-turation problem in biomass estimation. Int. J. Remote Sens. 25 (19), 3999–4014.
Mutanga, O., Skidmore, A.K., 2007. Red edge shift and biochemical content in grass ca-nopies. ISPRS J. Photogramm. Remote Sens. 62, 34–42.
Neuwirthová, E., Lhotáková, Z., Albrechtová, J., 2017. The effect of leaf stacking on leaf reflectance and vegetation indices measured by contact probe during the season. Sensors 17, 1202.
Obeidat, W., 2017. Genetic Variation for Chilling Stress and Spectral Reflectance in Short-season Maize. Doctoral dissertation. The University of Guelph.
Ollinger, S.V., 2011. Sources of variability in canopy reflectance and the convergent properties of plants. New Phytol. 189, 375–394.
Peñuelas, J., Filella, I., Biel, C., Serrano, L., Save, R., 1993. The reflectance at the 950–970 nm region as an indicator of plant water status. Int. J. Remote Sens. 14 (10), 1887–1905.
Penuelas, J., Baret, F., Filella, I., 1995. Semi-empirical indices to assess carotenoids/chlorophyll a ratio from leaf spectral reflectance. Photosynthetica 31, 221–230.
Porra, R.J., Thompson, W.A., Kriedemann, P.E., 1989. Determination of accurate ex-tinction coefficients and simultaneous equations for assaying chlorophylls a and b extracted with four different solvents: verification of the concentration of chlorophyll standards by atomic absorption spectroscopy. Biochim. Biophys. Acta Bioenerg. 975, 384–394.
Potůčková, M., Červená, L., Kupková, L., Lhotáková, Z., Lukeš, P., Hanuš, J., Novotný, J., Albrechtová, J., 2016. Comparison of reflectance measurements acquired with a contact probe and an integration sphere: implications for the spectral properties of vegetation at a leaf level. Sensors 16, 1801.
Prasad, B., Carver, B.F., Stone, M.L., Babar, M.A., Raun, W.R., Klatt, A.R., 2007. Genetic analysis of indirect selection for winter wheat grain yield using spectral reflectance indices. Crop Sci. 47, 1416–1425.
Pu, R., Gong, P., Biging, G.S., Larrieu, M.R., 2003. Extraction of red edge optical para-meters from Hyperion data for estimation of forest leaf area index. IEEE Trans. Geosci. Remote Sens. 41, 916–921.
Pukacki, P.M., Kamińska-Rożek, E., 2005. Effect of drought stress on chlorophyll a fluorescence and electrical admittance of shoots in Norway spruce seedlings. Trees 19, 539–544.
R Core Team, 2017. R: A Language and Environment for Statistical Computing. R Foundation for Statistical Computing, Vienna, Austria. http://www.R-project.org/.
Rautiainen, M., Lukeš, P., Homolová, L., Hovi, A., Pisek, J., Mõttus, M., 2018. Spectral properties of coniferous forests: a review of in situ and laboratory measurements. Remote Sens. 10, 207.
Richardson, A.D., Berlyn, G.P., 2002. Changes in foliar spectral reflectance and chlor-ophyll fluorescence of four temperate species following branch cutting. Tree Physiol. 22, 499–506.
Rincent, R., Charpentier, J.P., Faivre-Rampant, P., Paux, E., Le Gouis, J., Bastien, C., Segura, V., 2018. Phenomic Selection: A Low-cost and High-throughput Alternative to Genomic Selection. bioRxiv, pp. 302117.
Rock, B.N., Hoshizaki, T., Miller, J.R., 1988. Comparison of in situ and airborne spectral measurements of the blue shift associated with forest decline. Remote Sens. Environ. 24, 109–127.
Rondeaux, G., Steven, M., Baret, F., 1996. Optimization of soil-adjusted vegetation in-dices. Remote Sens. Environ. 55, 95–107.
Santiso, X., López, L., Gilbert, K.J., Barreiro, R., Whitlock, M.C., Retuerto, R., 2015. Patterns of genetic variation within and among populations in Arbutus unedo and its relation with selection and evolvability. Perspect. Plant Ecol. 17, 185–192.
Schaepman-Strub, G., Schaepman, M.E., Painter, T.H., Dangel, S., Martonchik, J.V., 2006. Reflectance quantities in optical remote sensing—definitions and case studies. Remote Sens. Environ. 103 (1), 27–42.
Sievert, C., Parmer, C., Hocking, T., Chamberlain, S., Ram, K., Corvellec, M., 2016. plotly: Create Interactive Web Graphics via 'plotly.js'. 13 R Package Version 3.4.
Soukupova, J., Rock, B.N., Albrechtova, J., 2002. Spectral characteristics of lignin and soluble phenolics in the near infrared-a comparative study. Int. J. Remote Sens. 23, 3039–3055.
Stimson, H.C., Breshears, D.D., Ustin, S.L., Kefauver, S.C., 2005. Spectral sensing of foliar water conditions in two co-occurring conifer species: *Pinus edulis* and *Juniperus monosperma*. Remote Sens. Environ. 96 (1), 108–118.
Ustin, S.L., Gamon, J.A., 2010. Remote sensing of plant functional types. New Phytol. 186, 795–816.
Virlet, N., Costes, E., Martinez, S., Kelner, J.-J., Regnard, J.-L., 2015. Multispectral air-borne imagery in the field reveals genetic determinisms of morphological and tran-spiration traits of an apple tree hybrid population in response to water deficit. J. Exp. Bot. 66, 5453–5465 erv355.
Vogelmann, J.E., Rock, B.N., Moss, D.M., 1993. Red-edge spectral measurements of sugar maple leaves. Int. J. Remote Sens. 14 (9), 1563–1575.
Wellburn, A.R., 1994. The spectral determination of chlorophylls a and b, as well as total carotenoids, using various solvents with spectrophotometers of different resolution. J. Plant Physiol. 144, 307–313.
Wickham, H., 2009. ggplot2: Elegant Graphics for Data Analysis. Springer-Verlag, New York.
Wong, C.Y., Gamon, J.A., 2015. The photochemical reflectance index provides an optical indicator of spring photosynthetic activation in evergreen conifers. New Phytol. 206, 196–208.
Yamasaki, E., Altermatt, F., Cavender-Bares, J., Schuman, M.C., Zuppinger-Dingley, D., Garonna, I., Schneider, F.D., Guillén-Escribá, C., van Moorsel, S.J., Hahl, T., Schmid, B., Schaepman-Strub, G., Schaepman, M.E., Shimizu, K.K., 2017. Genomics meets remote sensing in global change studies: monitoring and predicting phenology, evolution and biodiversity. Curr. Opin. Environ. Sustain. 29, 177–186.
Zarco-Tejada, P.J., Miller, J.R., Noland, T.L., Mohammed, G.H., Sampson, P.H., 2001. Scaling-up and model inversion methods with narrowband optical indices for chlorophyll content estimation in closed forest canopies with hyperspectral data. IEEE Trans. Geosci. Remote Sens. 39, 1491–1507.